

# Standardized Index of Shape (SIS): a quantitative DCE-MRI parameter to discriminate responders by non-responders after neoadjuvant therapy in LARC

Antonella Petrillo · Roberta Fusco · Mario Petrillo · Vincenza Granata ·  
Mario Sansone · Antonio Avallone · Paolo Delrio · Biagio Pecori ·  
Fabiana Tatangelo · Gennaro Ciliberto

Received: 10 July 2014 / Revised: 15 December 2014 / Accepted: 19 December 2014 / Published online: 11 January 2015  
© European Society of Radiology 2015

## Abstract

**Objectives** To investigate the potential of DCE-MRI to discriminate responders from non-responders after neoadjuvant chemo-radiotherapy (CRT) for locally advanced rectal cancer (LARC). We investigated several shape parameters for the time-intensity curve (TIC) in order to identify the best combination of parameters between two linear parameter classifiers. **Methods** Seventy-four consecutive patients with LARC were enrolled in a prospective study approved by our ethics committee. Each patient gave written informed consent. After surgery, pathological TNM and tumour regression grade (TRG) were estimated. DCE-MRI semi-quantitative analysis (sqMRI) was performed to identify the best parameter or parameter combination to discriminate responders from non-

responders in response monitoring to CRT. Percentage changes of TIC shape descriptors from the baseline to the presurgical scan were assessed and correlated with TRG. Receiver operating characteristic analysis and linear classifier were applied.

**Results** Forty-six patients (62.2 %) were classified as responders, while 28 subjects (37.8 %) were considered as non-responders. sqMRI reached a sensitivity of 93.5 % and a specificity of 82.1 % combining the percentage change in Maximum Signal Difference ( $\Delta$ MSD) and Wash-out Slope ( $\Delta$ WOS), the Standardized Index of Shape (SIS).

**Conclusions** SIS obtains the best result in discriminating responders from non-responders after CRT in LARC, with a cut-off value of  $-3.0$  %.

A. Petrillo (✉) · R. Fusco · M. Petrillo · V. Granata  
Division of Radiology, Department of Diagnostic Imaging, Radiant and Metabolic Therapy, “Istituto Nazionale Tumori Fondazione Giovanni Pascale – IRCCS”, Via Mariano Semmola, 80131 Naples, Italy  
e-mail: a.petrillo@istitutotumori.na.it

M. Sansone  
Department of Biomedical, Electronics and Telecommunications Engineering, University “Federico II” of Naples, via Claudio no.21, 80132 Naples, Italy

A. Avallone  
Division of Gastrointestinal Medical Oncology, Department of Abdominal Oncology, “Istituto Nazionale Tumori Fondazione Giovanni Pascale – IRCCS”, Via Mariano Semmola, 80131 Naples, Italy

P. Delrio  
Division of Gastrointestinal Surgical Oncology, Department of Abdominal Oncology, “Istituto Nazionale Tumori Fondazione Giovanni Pascale – IRCCS”, Via Mariano Semmola, 80131 Naples, Italy

B. Pecori  
Division of Radiotherapy, Department of Diagnostic Imaging, Radiant and Metabolic Therapy, “Istituto Nazionale Tumori Fondazione Giovanni Pascale – IRCCS”, Via Mariano Semmola, 80131 Naples, Italy

F. Tatangelo  
Division of Diagnostic Pathology, Department of Diagnostic and Laboratory Pathology, “Istituto Nazionale Tumori Fondazione Giovanni Pascale – IRCCS”, Via Mariano Semmola, 80131 Naples, Italy

G. Ciliberto  
“Istituto Nazionale Tumori Fondazione Giovanni Pascale – IRCCS”, Via Mariano Semmola, 80131 Naples, Italy

### Key Points

- DCE-MRI shape descriptors are investigated to assess pre-operative CRT response in LARC.
- Identification of the best TIC shape descriptors combination through a linear classifier.
- Identification of a single MRI index to predict neoadjuvant treatment response.

**Keywords** LARC · Neoadjuvant chemo-radiotherapy · DCE-MRI · Semi-quantitative analysis · Treatment response assessment

### Introduction

Rectal cancer is a frequent malignancy in both men and women, accounting for 40,290 new cases in the USA in 2012 [1]. Despite the efforts made to introduce screening programs, most patients are diagnosed at a locally advanced stage of the disease (T3-T4, Nx, Mx). Total mesorectal excision (TME) combined with preoperative radiation therapy and concurrent chemotherapy (CRT) is the current standard for locally advanced rectal cancer (LARC) [2, 3]. TME is associated with significant morbidity and functional complications; evolving conservative treatment strategies are being developed for patients with early rectal cancer at diagnosis and patients with significant/complete tumour regression after preoperative CRT. A further conservative strategy has been to adopt a ‘wait and see’ policy, omitting surgery when a complete clinical response is obtained after preoperative CRT. This strategy has the advantage of reducing morbidity and provides a ‘true’ organ-sparing approach, considering that sphincter preservation without adequate function has questionable benefit. A major challenge for organ-sparing treatments after good pathological response in LARC is the selection of patients suitable for such an approach. Morphological MRI evaluation (mMRI) is considered the best available tool for LARC staging, allowing an accurate evaluation of the disease extent, up to, beyond and over the mesorectal fascia, and of the lymph node involvement [4]. However, there are some limitations in depicting changes after CRT through morphological MRI alone. A favourable tumour response may not correspond to an appreciable tumour size reduction. Moreover, it is difficult to differentiate between post-radiation fibrosis and fibrosis containing viable tumour remnants. Studies are therefore focusing on the potential added benefit of functional and/or quantitative methods of MR image evaluation. Dynamic contrast-enhanced MRI (DCE-MRI) has proven useful in detecting residual tumour after CRT [5–9]: leaky capillaries associated with tumour neovascularization determine a rapid gadolinium uptake and an early wash-out, which correlate with the vascular endothelial growth factor (VEGF)

expression and micro vessel density (MVD) [10–12]. DCE-MRI evaluation can be assessed through time intensity curve (TIC) analysis performed using three different approaches: qualitative DCE-MRI, quantitative DCE-MRI and semi-quantitative DCE-MRI based on pattern analysis. Qualitative DCE-MRI involves the visual inspection and classification of TIC in accordance with the scheme proposed by Daniel et al. [7]. The shape of the curve can summarize the angiogenic characteristics of the tumour, which is typically divided into two phases: wash-in (contrast agent enhancement) and wash-out (contrast agent excretion). A high or low slope in the first phase or wash-in phase (WI) suggests high or low angiogenesis, respectively [13]. With regard to the second phase or wash-out phase (WO), a steep decline (Type 3) corresponds to higher vascular permeability. A continuous rise (Type 1 or persistent enhancement) represents lower permeability. A stable curve (Type 2 or plateau) also depicts higher permeability when its signal intensity does not reach a plateau [14]. The main drawback of the qualitative approach is the operator dependence. Quantitative DCE-MRI can be achieved by applying an adequate pharmacokinetic model to the TIC [15]. This approach can yield parameters with a direct physiological interpretation. However, quantitative DCE-MRI involves many critical issues: accurate measurement of the arterial input function, accurate quantification of gadolinium, choice of an adequate model, and accurate estimation of tracer kinetic parameters [16]. Semi-quantitative DCE-MRI consists of the calculation of opportune TIC shape descriptors providing summary information, roughly related to the pathophysiology of the cancer. This approach could be more robust in clinical settings, since many critical issues of quantitative analysis are attenuated. However, semi-quantitative parameters do not have a direct interpretation in terms of physiological characteristics [17, 18]. Previous DCE-MRI studies have investigated shape descriptors for non-invasive response assessment in various malignancies, including rectal cancer [12, 13, 17, 18]. These initial investigations have focused on several outcome variables such as response, correlation with angiogenesis markers, and overall presence of tumour response, by classifying patients empirically into ‘responder’ and ‘not responder’ based on T stage or clinical down-staging. However, patients with complete tumour regression based on tumour regression grade (TRG) represent a distinct subset with a particularly favourable outcome, thus suggesting that further therapy could be tailored according to tumour staging after CRT. Moreover, individualizing a single parameter, easily translatable in clinical practice, through which one can discriminate responder from non-responder patients after CRT still remains a challenge.

The aim of this study was to investigate dynamic contrast-enhanced MRI (DCE-MRI) with the purpose of discriminating responders from non-responders after CRT for LARC and to investigate several shape parameters for the time-intensity

curve (TIC) in order to identify the best parameters combination.

## Materials and methods

### Patient selection

Seventy-four consecutive patients (22 women and 52 men) with a median age of 62 years (range 29–76 years) were enrolled in this prospective study from March 2007 to July 2013. All patients had a biopsy-proven rectal adenocarcinoma. Endorectal ultrasound, MRI of the liver and pelvis, CT of the abdomen and pelvis, and chest x-ray were used as staging procedures. Inclusion criteria were: patients with clinical T4, nodal involvement or T3 N0 with a tumour location  $\leq 5$  cm from the anal verge or a circumferential resection margin of  $\leq 5$  mm, defined by MRI. Exclusion criteria were: inability to give informed consent, previous rectal surgery, and contraindications to MRI or to MR contrast media. All patients were enrolled within the phase I-II prospective trial described in Avallone et al. [19], which was approved by the Independent Ethics Committee of our institution. All patients provided written informed consent to participate in the trial.

### Neoadjuvant therapy

External radiation therapy was performed using a three-field technique (one posterior-anterior and two lateral fields). Standard fractions of 1.8 Gy/day to the reference point were given five times a week up to a total dose of 45 Gy. Two different regimens were carried out for the concomitant chemotherapy. Fifty-four patients received bi-weekly bevacizumab at 5 mg/kg plus three bi-weekly cycles of oxaliplatin at 100 mg/m<sup>2</sup> and raltitrexed at 2.5 mg/m<sup>2</sup> on day 1, and levo-folinic acid at 250 mg/m<sup>2</sup>, and 5-fluorouracil at 800 mg/m<sup>2</sup> on day 2 [2, 19]. The 20 remaining subjects received capecitabine at a dose of 825 mg/m<sup>2</sup> twice a day, 5 days a week, for 5 weeks.

### MRI data acquisitions

All patients underwent DCE-MRI examination before and after CRT (90 days on average, range 86–94 days). Imaging was performed with a 1.5 T scanner (Magnetom Symphony, Siemens Medical System, Erlangen, Germany) equipped with a phased-array body coil. Patients were placed in a supine, head-first position. Mild rectal lumen distension was achieved with 60–90 mL of undiluted ferumoxil (Lumirem, Guerbet, Roissy CdG Cedex, France) suspension introduced per rectum [20]. Precontrast coronal T1w 2D turbo spin-echo images and sagittal and axial T2w 2D turbo spin-echo images of the pelvis were obtained for the mMRI. Subsequently, axial, dynamic,

contrast-enhanced T1w, FLASH 3D gradient-echo images were acquired for the sqMRI and for pattern analysis. We obtained one sequence before and ten sequences, without any delay, after the intravenous (IV) injection of 2 ml/kg of a positive, gadolinium-based paramagnetic contrast medium (Gd-DOTA, Dotarem, Guerbet, Roissy CdG Cedex, France). The contrast medium was injected using Spectris Solaris® EP MR (MEDRAD Inc., Indianola, PA, USA), with a flow rate of 2 ml/s, followed by a 10-ml saline flush at the same rate. Temporal resolution was 0.58 min, corresponding to 35 s (as reported in Table 1). Total acquisition time for pre-contrast and ten post-contrast sequences was 6.4 minutes. Then, sagittal, axial and coronal post-contrast T1w 2D turbo spin-echo images, with and without fat saturation, were obtained (Table 1). The axial images were acquired without any angulation. Axial T1-w pre- and post-contrast sequences were acquired at the same position as the T2-w sequence. MRI total acquisition time was around 30 minutes.

### Image data analysis

Image assessment was performed in a single reading session for each patient by consensus of two gastrointestinal radiologists (A.P. and V.G.) with 18 years and 5 years of experience, respectively, in reading pelvic MR images. mMRI evaluation on post-CRT T2w images followed the criteria set out by Dresen et al. [21]. Lesions showing a complete disappearance of the tumour or residual tumour surrounded by a dark, intact bowel wall were classified as T0-T2. Lesions exhibiting a residual isointense mass penetrating the rectal wall and/or the mesorectal fascia and/or the surrounding organs were classified as T3-T4. Since MRI cannot distinguish between fibrosis with and without tumour [20], patients with a thickened but hypo-intense rectal wall were also categorized as T3. For morphological MRI evaluation, tumour volumes were calculated by manually tracing the tumour boundaries slice by slice on conventional T2-weighting. Whole-tumour volume was calculated by considering the total number of pixels (slice by slice) and multiplying this by pixel size in mm<sup>2</sup>. For semi-quantitative analysis of MRI evaluation, in order to take into account tumour heterogeneity, the radiologists, based on pre-contrast T1-weighted images using the T2-weighted images as a guide, manually drew regions of interests (ROIs) along contours of the tumour, covering the whole lesion with exclusion of the peripheral fat, artefact and blood vessels. Histograms of pixel data were obtained from all acquired tumour slices, and median values and standard deviation were recorded for each study. The semi-quantitative analysis was performed on ROIs previously described. For each pixel, TICs were obtained and for each TIC, eight shape descriptors (Fig. 1) were computed using the approach previously reported in another of our papers [17]: the maximum signal difference (MSD), the time to the knee between the WI and WO

**Table 1** Pulse sequence parameters on MR studies

Sequence	Orientation	TR/TE/FA (ms/ms/deg.)	AT (min)	FOV (mmxmm)	Matrix	ST/Gap (mm/mm)	TF
T1w 2D TSE	Coronal	499/13/150	2.36	450×450	256×230	3 / 0	3
T2w 2D TSE	Sagittal	4820/98/150	4.17	260×236	256×139	3 / 0	13
T2w 2D TSE	Axial	3970/98/150	3.48	270×236	256×157	3 / 0	13
T1w FLASH 3D	Axial	9.8/4.76/25	0.58	330×247	256×192	3 / 0	/
T1w FLASH 3D	Axial	9.8/4.76/25	0.58×10	330×247	256×192	3 / 0	/
T1w 2D TSE	Sagittal	538/13/150	2.35	250×250	256×230	3 / 0	5
T1w 2D TSE	Coronal	538/13/150	2.52	250×250	256×230	3 / 0	5
T1w 2D TSE	Axial	450/12/150	2.31	270×236	256×202	3 / 0	5

Note: TR = repetition time, TE = echo time, FOV = field of view, FA = flip angle, ST = slice thickness, TF = turbo factor, AT = acquisition time

segments (TTP), the WI slope (WIS), the WO slope (WOS), the WI intercept (WII), the WO intercept (WOI), the WOS/WIS ratio, the WOI/WII ratio. Each descriptor's median value and standard deviation were obtained and the percentage changes between pre- and post-treatment  $\Delta X = (X_{pre} - X_{post})/X_{pre}$  were calculated ( $X$  is the generic shape descriptor). Semi-quantitative analyses were carried out using the Matlab R2007a software (The Math-Works Inc., Natick, MA, USA).

#### Surgical approach and evaluation of pathological response

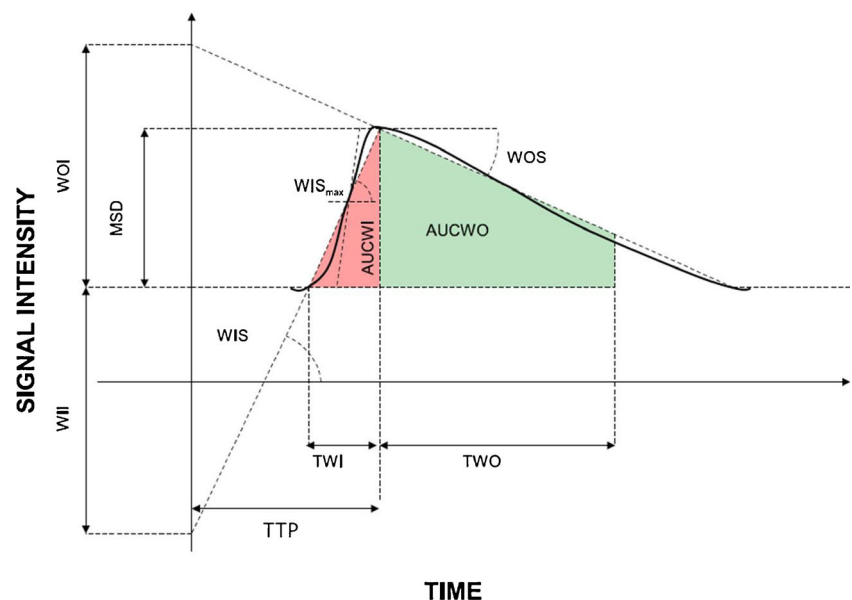
All patients underwent total mesorectal excision after completing CRT (58 days on average, range 48–66 days). An anterior resection or an abdominal-perineal resection was performed based on the results of post-CRT restaging. The surgical specimens containing the tumour were processed and evaluated by a single pathologist who was not aware of either the clinical or the MRI findings. The circumferential resection margin was examined by sampling a 1-mm thick slice [22]

and was defined as positive if the tumour residuals were found  $\leq 1$  mm from the margin. Lymph nodes were examined by the manual dissection method [11]. The mandard TRG scoring system was used [23]: TRG 1 means a complete response with absence of residual cancer and fibrosis extending through the wall. TRG 2 is the presence of residual cancer cells scattered through the fibrosis. TRG 3 corresponds to an increased number of residual cancer cells, with predominant fibrosis. TRG 4 indicates residual cancer outgrowing fibrosis. TRG 5 is the absence of regressive changes. Patients with a TRG 1 or 2 score were considered as responders, whereas the remaining patients (TRG 3, 4, or 5) were classified as non-responders [12].

#### Statistical analysis

To assess the influence of the two chemotherapy regimens on the results, we compared the proportion of responders with the non-responders in the two different chemotherapy groups by means of a chi-square test. The univariate

**Fig. 1** Semi-quantitative analysis: illustration of the parameters calculated from the TIC





analysis was carried out to evaluate the ability of single-shape descriptors to discriminate responders from non-responders. To this aim, non-parametric tests for paired data (Wilcoxon test) were used to verify differences before and after CRT. The tests were applied to each shape descriptor obtained as median value and standard deviation. The Mann-Whitney test for unpaired data was used to verify statistically significant differences in  $\Delta X$  of each shape descriptor between the two groups (responders and non-responders). Moreover, receiver operating characteristic (ROC) curves were calculated using percentage change of tumour volume and percentage change for each DCE-MRI shape parameter. For each ROC, the area under the curve (AUROC) was calculated [24]. The AUROCs were compared using nonparametric methods [25] and optimal thresholds were obtained maximizing the Youden index [26]. Multivariate analysis was performed to calculate the best combination of shape descriptors to discriminate responders from non-responders. We considered the linear classifiers that can be generated from independent pairs of the eight shape descriptors. For any two paired parameters,  $\Delta X_1$  and  $\Delta X_2$  considered as percentage change, ROCs curves were computed by applying the method referenced above to the linear combination  $p = \Delta X_1 \cos\theta - \Delta X_2 \sin\theta$ , for  $\theta$  varying from  $-180^\circ$  to  $180^\circ$  in 1-degree increments. For each  $\theta$ , the AUROC was computed by trapezoidal rule integration. The best possible linear classifier was then determined by maximizing the AUROC as a function of  $\theta$  and was indicated as  $\Delta X_1$  and as  $\Delta X_2$  [27]. A P-value  $<0.05$  was considered significant for all tests. All analyses were performed using Statistics Toolbox of Matlab R2007a (The Math-Works Inc., Natick, MA, USA).

## Results

### Population

All patients in our series had rectal adenocarcinomas, G2 graded, with an intact and complete mesorectum after total excision. Fifteen patients were pathologically classified as T0 (20.3 %), ten as T1 (13.5 %), 27 as T2 (36.5 %), 17 as T3 (23.0 %), and five as T4 (6.7 %). There were 22 patients with a TRG 1 (29.7 %), 24 with a TRG 2 (32.4 %), 21 with a TRG 3 (28.4 %), five with a TRG 4 (6.8 %), and two with a TRG 5 (2.7 %). According to morphological MRI on T2w images, ten (13.5 %) patients were staged as T0, 22 (29.7 %) as T2, 38 (51.4 %) as T3, and four (5.4 %) as T4. The Chi-square test, used to evaluate the influence of two different chemotherapy regimens, showed that the therapy regimen did not affect the proportions in responder and non-responder patients.

*Univariate analysis of DCE-MRI shape descriptors* On univariate analysis, the Wilcoxon test showed statistically significant differences before and after CRT in responders for MSD and WOS median values (Table 2, Fig. 2). However, in non-responders, no statistically significant difference was observed for each one of the eight descriptors (Table 2). Statistically significant differences between responders and non-responders in the percentage change of the MSD and WOS were also obtained with the Mann-Whitney test (Table 3).

Tumour volume morphological variation showed a low correlation between response and TRG with a sensibility and specificity, respectively, of 74 % and 67 % (33 % cut-off, AUROC 0.67). For DCE-MRI descriptors, the maximum AUROC was obtained for  $\Delta$ MSD and  $\Delta$ WOS, 0.73 and 0.81, respectively. The optimal cut-off value in  $\Delta$ MSD of  $-15.1$  % yields 74.0 % sensitivity and 70.4 % specificity; optimal cut-off value in  $\Delta$ WOS of 18.9 % gave a sensitivity of 80.4 % and a specificity of 77.8 %.

*Multivariate analysis of DCE-MRI shape descriptors* Among all ROC curves computed for each pair of the eight descriptors, the combination of  $\Delta$ MSD and  $\Delta$ WOS (blue ROC curve in Fig. 3a) yielded the best results. A combination of  $\Delta$ MSD and  $\Delta$ WOS gave an improvement in the AUROC (0.899) when compared to  $\Delta$ MSD and  $\Delta$ WOS alone (Fig. 3a). The linear classifier maximizing AUROC for  $\Delta$ MSD and  $\Delta$ WOS was given as  $0.7780 \cdot \Delta$ MSD +  $0.6157 \cdot \Delta$ WOS (Fig. 4). We defined this linear combination as the Standardized Index of Shape (SIS). The optimal cut-off value in SIS change was  $-3.0$  % (Youden Index). Sensitivity and specificity values were 93.5 % and 82.1 %, respectively, and positive and negative predictive values were 89.6 % and 88.5 %, respectively. The McNemar test [25] showed that SIS AUROC was significantly greater than tumour volume morphological variation AUROC (P-value  $<0.01$ ),  $\Delta$ MSD and  $\Delta$ WOS AUROC (P-value  $<0.05$ ). When the distributions of  $\Delta$ MSD,  $\Delta$ WOS and SIS values were compared distinguishing complete response (TRG=1) and non-complete response (TRG $\geq$ 2), the AUROCs were, respectively, 0.66, 0.61 and 0.72 (Fig. 3b). However, the SIS reached better results with a sensitivity of 71.2 % and specificity of 65.4 %. A large number of patients in the complete response group are needed to evaluate a significant statistical difference and to establish the optimal threshold to differentiate patients with a complete response.

## Discussion

Since histological down-staging is not always associated with tumour size reduction, mMRI alone is not considered conclusive in tumour-response evaluation after CRT in LARC [21]. The main drawback of morphological MRI is the discrimination of active tumour tissue by post-treatment fibrosis (Figs. 5

**Table 2** Semi-quantitative parameters: median values of responder and non-responder patients according to TRG criteria at two time points: pre and post neo-adjuvant therapy

Variable	Pre CRT responders	Post CRT responders	P-value*	Pre CRT non-responders	Post CRT non-responders	P-value*
MSD	1.51±0.9	0.80±0.84	<b>0.03</b>	0.7±0.6	1.0±0.9	0.06
TTP	210.0±53.7	245.00±43.39	0.10	210.0±44.3	280.0±47.6	0.10
WII	78.9±56.0	55.41±64.29	0.62	65.5±42.1	53.2±31.1	0.07
WOI	137.9±39.8	132.38±27.71	0.15	151.4±96.9	132.7±69.4	0.65
WIS	0.2±0.6	0.37±0.44	0.89	0.2±0.4	0.3±0.4	0.19
WOS	-0.03±1.4	-0.01±1.34	<b>0.03</b>	-0.02±1.6	-0.02±1.5	0.63
WOS/WIS	-0.05±18.3	-0.04±17.44	0.31	-0.1±17.3	-0.1±13.1	0.75
WOI/WII	1.3±5.0	1.42±4.61	0.51	1.5±5.1	1.9±5.8	0.08

Note: Data are median ± standard deviations; \* Wilcoxon test; MSD = maximum signal difference; TTP = time to peak; WII = wash-in intercept; WOI = wash-out intercept; WIS = wash-in slope; WOS = wash-out slope; CRT = chemo-radiation therapy

P value < 0.05 were indicated in bold to highlight the statistical significance

and 6). Our findings have confirmed that T2-weighted imaging volume assessment alone is not sufficiently accurate (74 % of sensibility and 67 % of specificity), not being able to discriminate between the persistence of viable tissue and the peritumoral fibrosis present after radiation therapy. Residual tumour within the fibrotic areas is frequently represented by small tumour nests, beyond the depiction level of morphological MRI [21]. According to T stage after CRT, Chen et al. [8] reported an overstaging of 38 % and an accuracy of 52 %. With regard to qualitative DCE-MRI, the main drawback remains ROI positioning, which makes the evaluation operator dependent [7]. At the same time, quantification through visual TIC inspection is not achievable, as it misses reproducible numerical data for comparison. According to our previous experience, when patients with a partial or complete response to CRT were included, we obtained a sensitivity, a specificity and an accuracy, respectively, of 79 %, 76 % and 78 %; while considering the performance of qualitative MRI evaluation in complete responders we reached a sensitivity, a specificity and

an accuracy, respectively, of 94 %, 76 % and 84 % [9]. To overcome the limitations related to visual inspection alone, the calculation of opportune TIC shape descriptors characterized the semiquantitative MRI analysis focusing on relationships that link tumour viability to angiogenesis. Zhang et al. [12] demonstrated the ability of 3T DCE-MRI to discriminate rectal carcinoma from normal tissue, showing a close relationships among functional parameters, VEGF and MVD expression. Lavini et al. [28], in order to classify the pixels according to benignity and malignancy, used the following features: maximum signal difference (sometimes referred as relative enhancement), TTP, maximum slope of increase, relative final slope and initial signal. Tuncbilek et al. [29] observed that TTP, wash-in intercept, and maximum enhancement were strongly correlated to MVD. Blomqvist et al. [30] proposed a TIC piecewise linear fitting reporting wash-out intercept as the parameter that significantly differentiated between malignant and benign lesions. Another developed approach is based on quantitative ‘model-based’ investigations that involve

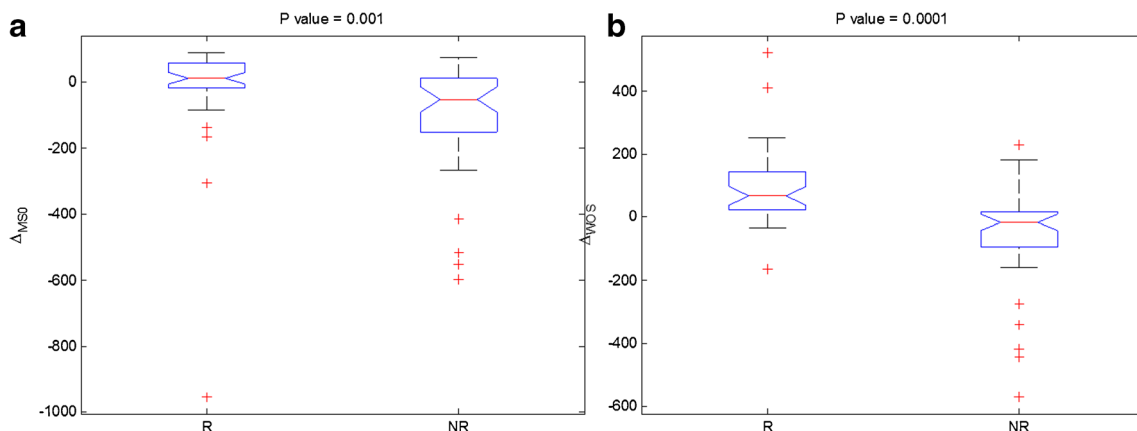


**Fig. 2** Box plots of  $\Delta_{MSD}$  (a) and  $\Delta_{WOS}$  (b) representing differences in distributions of responders (R) and non-responders (NR). The middle line is the median value. The inferior and superior extremes of the box correspond to the first and third quartile, respectively. The whiskers lines

correspond to values within 1.5 times the interquartile range from the ends of the box. Outlier data beyond the ends of the whiskers are displayed with a + sign

**Table 3** Semi-quantitative parameters: median values of percentage change ( $\Delta$ ) for each parameter in responder and non-responder patients according to TRG criteria

Variable	Responders	Non-responders	P-value
$\Delta$ MSD	10.15	-52.68	<b>0.001</b>
$\Delta$ TTP	-6.25	-14.29	0.57
$\Delta$ WII	32.70	25.10	0.52
$\Delta$ WOI	4.49	8.08	0.89
$\Delta$ WIS	-14.02	-42.49	0.24
$\Delta$ WOS	67.94	-16.67	<b>0.0001</b>
$\Delta$ WOS/WIS	16.64	-8.52	0.33
$\Delta$ WOI/WII	9.99	-4.74	0.06

Note:  $\Delta$  = percentage change between pre and post chemo-radiation treatment; MSD = maximum signal difference; TTP = time to peak; WII = wash-in intercept; WOI = wash-out intercept; WIS = wash-in slope; WOS = wash-out slope; CRT = chemo-radiation therapy  
 P value < 0.05 were indicated in bold to highlight the statistical significance

compartmental tracer kinetic modelling [15] and pixel-by-pixel estimation of kinetic features, through nonlinear regression. The latter has been introduced to better correlate quantitative ‘model-based’ results with physiological tissue properties. Kim et al. [31] showed that the  $K^{trans}$  parameter (contrast agent transfer constant between plasma space to extracellular extravascular space) had a large decrease in the mean value after CRT and this was associated with a good therapeutic response to CRT for LARC. However, being influenced by many factors, many different models are still present in the literature and their high output variability reflects a poor clinical reliability [8, 16, 18, 32]. Results of quantitative analysis to assess therapy response on 3T MR scanners are more promising, as was reported in the studies of Intven et al. [33] and Lim et al. [34]. As an alternative, Guo et al. [18] proposed a piecewise linear fitting of the TIC in evaluating pixel-by-pixel

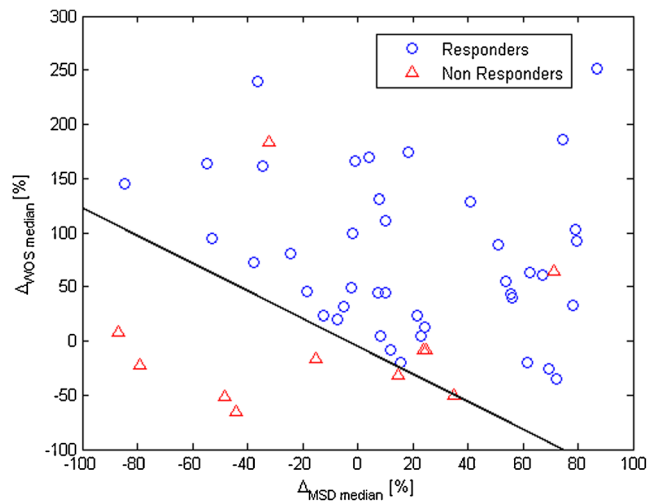


**Fig. 4** Scatter plot of  $\Delta$ WOS versus  $\Delta$ MSD for all patients. Responders were indicated by a blue round symbol and non-responders by a red triangular symbol. The linear classifier  $0.7780 * \Delta_{MSD} + 0.6157 * \Delta_{WOS} \geq -3.0$  %, provided a sensitivity of 93.5 %, a specificity of 82.1 %, a positive predictive value of 89.6 % and a negative predictive value of 88.5 %. Accuracy was 89.2 %

the osteosarcoma’s perfusion. Our semi-quantitative analysis employed this fitting adding the TIC normalization with the aim of eliminating the dependence on proton density, relaxivity and other equipment parameters, and to identify more suitable indexes in detecting CRT tumour response [17]. Statistically significant changes in discriminating responders from non-responders were obtained with two parameters, MSD and WOS – although an overlap was observed when each parameter was considered alone (Fig. 2). This determines a higher number of false positives and negatives. Therefore, we considered the hypothesis that a combination of descriptors could reduce this effect by optimizing sensibility, specificity and overall examination accuracy. To this aim, the linear combination of  $\Delta_{MSD}$  and  $\Delta_{WOS}$ , SIS, showed an improvement in sensitivity up to 93.5 %, with a specificity of

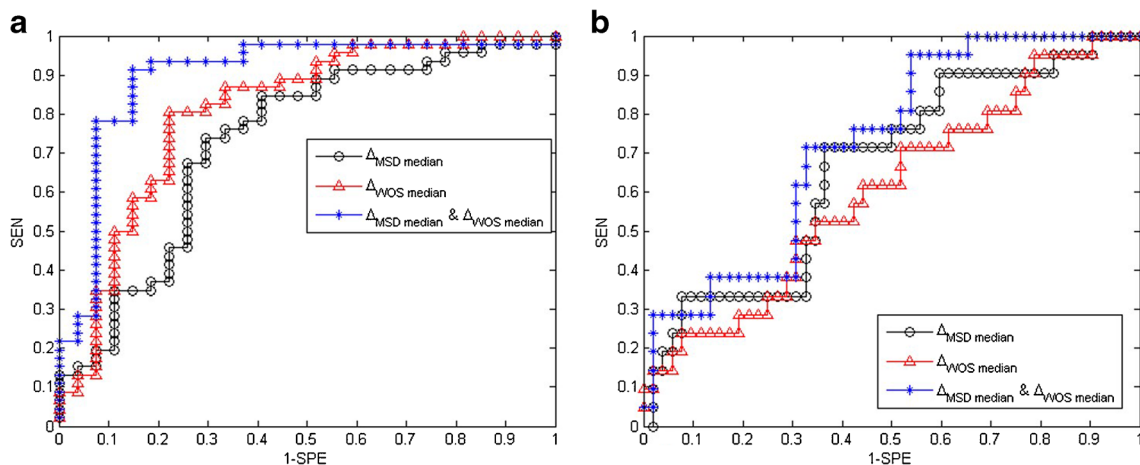


**Fig. 3** ROC analysis for  $\Delta_{MSD}$ ,  $\Delta_{WOS}$  and SIS in discriminating responders from non-responders (a). ROC analysis for  $\Delta_{MSD}$ ,  $\Delta_{WOS}$  and SIS in discriminating complete response from non-complete response (b)

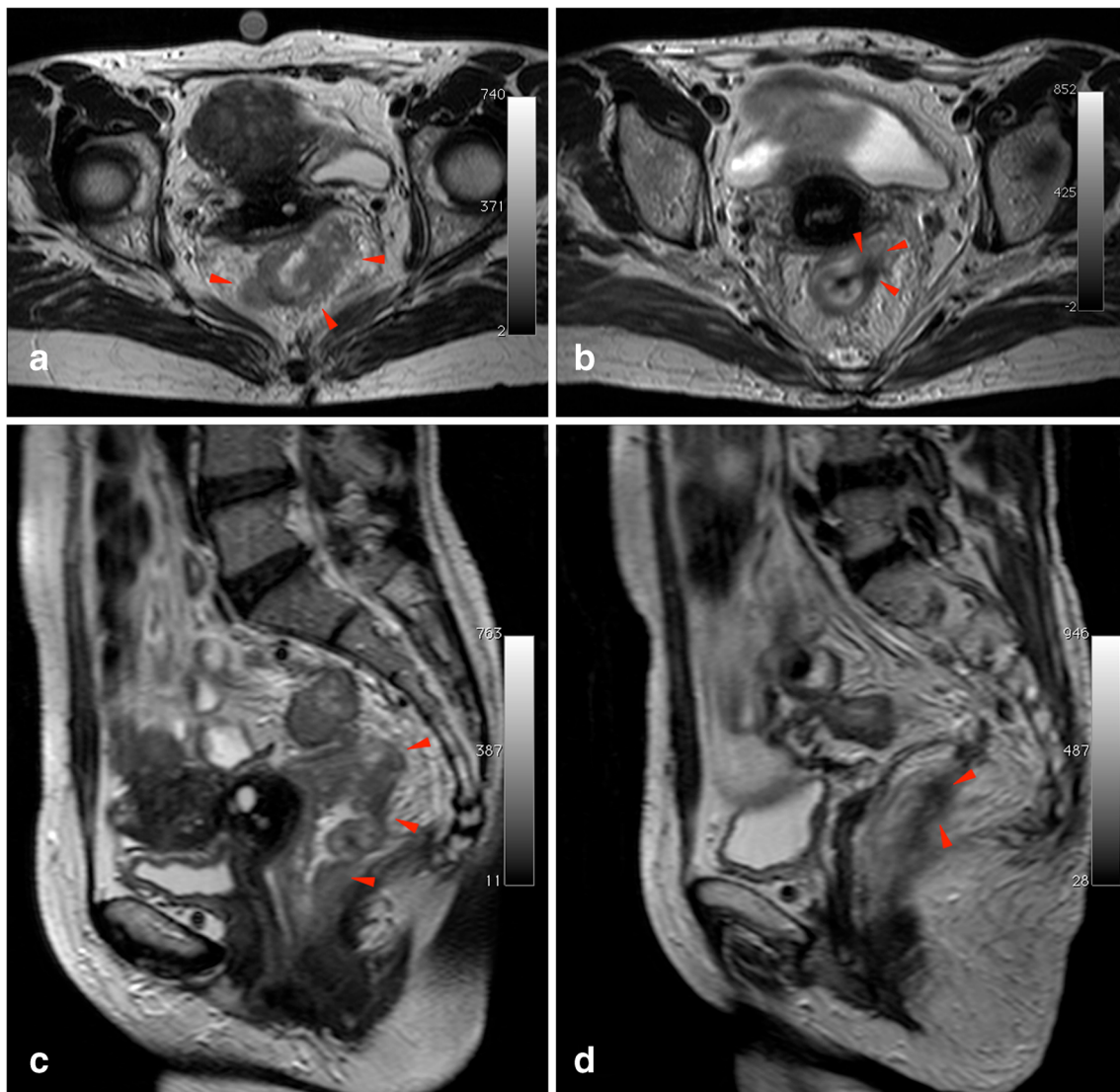


**Fig. 5** Patient no. 3. A case of overestimation in mMRI evaluation. Axial T2w images before (a) and after (b) CRT and sagittal T2w images before (c) and after (d) CRT. The morphological evaluation before CRT shows a heterogeneous irregular thickening along the entire rectal wall spreading into the perirectal fat (a, arrowheads). After CRT, a hypointense spiculated area with thin digitations is still clearly visible into the

perirectal fat (b, arrowheads). On the sagittal scan obtained before CRT multiple irregular rectal wall thickenings are shown (c, arrowheads). After CRT, a hypointense area with thickening of the rectal wall and straining into perirectal fat (d, arrowheads) was identified as a residual tumour probably mixed with fibrous tissue

82.1 % with relevant gains with respect to  $\Delta_{\text{MSD}}$  (+20.1 % in sensitivity and +11.7 % in specificity) and  $\Delta_{\text{WOS}}$  considered alone (+13.1 % in sensitivity and +4.3 % in specificity). SIS improved the negative predictive value to 88.5 % and the positive predictive value to 89.6 %. Our proposed matched index showed interesting results in re-staging LARC after CRT, providing a cut-off of  $-3.06$  %, which was able to accurately separate responders from non-responders. No similar studies are present in the literature that focus on the matching of multiple shape descriptors with the aim of obtaining a one 'stop shop' index that is robust, easy to apply and able to produce adequate performance when directly applied in clinical practice. The most attractive 'ultimate challenge' could be to boost the accuracy of MRI examinations integrating DCE-

MRI with DWI. The latter is a potential biomarker able to predict response to CRT [35–41], since pre-treatment apparent diffusion coefficient (ADC) and its changes correlate with down-staging. Recent studies have investigated the potential of DWI to assess therapy response in LARC: Cai et al. [38] showed that AUROC, for identification of a complete response after neoadjuvant therapy, was low for ADC (equal to 0.66 at 3T MRI and 0.64 at 1.5T MR scanner); they concluded that ADC measurements are not accurate for assessment of complete response. Genovesi et al. [39] showed that the diagnostic accuracy of the mean ADC increase, to discriminate the complete response group from the non-complete response group, was significantly higher than the mean tumour volume reduction (0.913 vs. 0.658;  $p=0.022$ ), concluding that



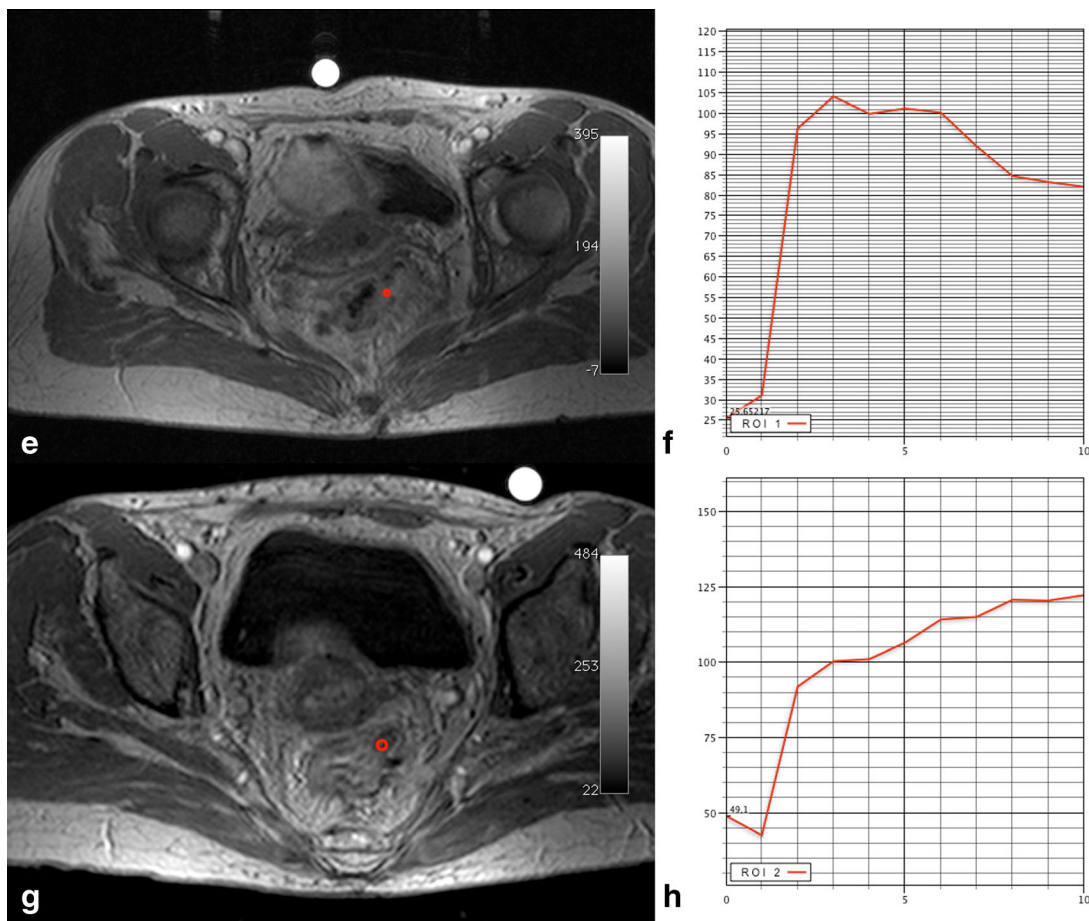


**Fig. 6** Patient no. 3, a case of correct sqMRI estimation. Axial T1w, contrast-enhanced scans obtained before (e), and after (g) CRT. Qualitative DCE-MRI based on TIC evaluation analysis obtained from the ROIs drawn before (f) and after (h) CRT. TIC confirms the perirectal infiltration

visible on the MR scan (e), showing a rapid contrast intake and a fast discharge (g). After CRT there is no fast contrast uptake identified on the TIC analysis, suggesting that the hypointense tissue is mainly due to the CRT-induced fibrosis

the mean ADC increase appears to be a reliable tool for differentiating complete response from non-complete response after CRT. Wu et al. [40] have performed a meta-analysis showing that MRI is an accurate tool in predicting pathological response after preoperative therapy in patients with LARC but suggested performing MRI with 3T devices, which might be sensitive enough to identify responders; moreover it is shown that the addition of DWI to T2-weighted imaging had a non-significant improvement in sensitivity, which deserves further investigation. Song et al. [41] reported that, utilizing 3T MR systems, the increase in signal-to-noise ratio (SNR) provided by these machines offers increased DWI quality and improvements to ADC maps, they reported that adding DWI to T2WI is helpful for detecting viable tumours after neoadjuvant CRT compared with T2 weighted imaging alone or PET in patients with LARC. The findings are still controversial; therefore, future investigations are desirable. A crucial point becomes apparent: the need to improve the diagnostic accuracy of perfusion studies with DCE-MRI and DWI. Therefore, before proceeding to integrate these different techniques we focused on developing an effective DCE-MRI approach.

Our data, if obtained during therapy and if supported by stronger numerical evidence, could offer several opportunities: SIS could be used to distinguish pathological complete responders from partial responders or non-responders in order to tailor neoadjuvant therapy on single subject response, to treat full responders with less extensive surgery or even to skip immediate surgery and to follow a wait-and-watch strategy through a strict follow-up program based on a complete response assessed by clinical and imaging analysis: endoscopic, DCE-MRI, DW-MRI and [ $^{18}\text{F}$ ]-fluorodeoxyglucose positron emission tomography (PET) studies. Today, PET evaluation is considered the best technique for assessing CRT response in LARC, and the most widely used in assisting physicians when planning optimal treatment. Cascini et al. [42] performed a PET evaluation based on the maximum variation of the standardized uptake value ( $\Delta\text{SUV}$ ) optimal threshold value of  $-42\%$  and identified 13 of 15 non-responders with a specificity of  $87\%$ . Although PET provides a tool to monitor tumour glucose metabolism, the method is less well suited to the study of tumour-associated angiogenesis or perfusion because of the ‘uncoupling’ of blood flow and glucose

metabolism that has been observed to occur in human tumours [43]. Moreover, low spatial resolutions coupled with ‘respiratory artefacts’ have a considerable impact on overall evaluation, drawbacks that have less impact on image assessment of DCE-MRI analysis.

Our study has certain limitations: the intra-observer variability was not assessed, but two radiologists evaluated the images by consensus and in a single session per patient. No precautions were taken to avoid bowel movements, nor was the administration of butylscopolamine, dicyclomine, glucagon or similar drugs carried out, because a volumetric analysis was performed thus minimizing errors due to caused voxel misalignments. The semi-quantitative approach used takes inspiration from studies on breast and osteosarcoma tumours, where leaky capillaries associated with tumour neovascularization determine rapid gadolinium tissue uptake and early washout, which correlate with VEGF and MVD [10–12]. However, being rapid growing, colorectal carcinomas similar to breast tumour and most malignant tumours for their biological characteristics, using their contrast kinetics on MRI can be depicted by DCE-MRI [8–11].

In conclusion, our study proposes a ‘surrogate angiogenic marker’, SIS, as a simple objective method, easily transferable to clinical routine and able to assess tumour response to CRT through a reproducible semi-quantitative estimation of tumour blood perfusion. SIS is the first pattern analysis MRI index suitable for establishing the response to CRT in LARC patients. We identified a well defined threshold value of SIS, able to differentiate responders (TRG 1 or 2) from non-responders (TRG 3, 4, or 5), allowing the prediction of a pathologically good response after neoadjuvant treatment. The future endpoint could be the analysis of the inter- and intra-operator variability; the development of SIS evaluation software, easy to use and able to guarantee a user-friendly experience for the operator; a comparison of SIS with the SUV obtained in PET is desirable with data integration, performed during intermediate therapy time points, leading to a tailored CRT. Lastly, it could allow the identification of a defined threshold value of SIS to differentiate pathological complete responders (TRG 1) from other responders (TRG > 2) that we could use to increase single TRG subgroups.

**Acknowledgments** The scientific guarantor of this publication is Dr. Antonella Petrillo. The authors of this manuscript declare no relationships with any companies, whose products or services may be related to the subject matter of the article. The authors state that this work has not received any funding. One of the authors has significant statistical expertise. Institutional Review Board approval was obtained. Written informed consent was obtained from all subjects (patients) in this study. Approval from the institutional animal care committee was not required because there are no animal subjects in this study. No study subjects or cohorts have been previously reported. Methodology: Prospective, diagnostic study, performed at one institution.

## References

1. Siegel R, Naishadham D, Jemal A (2012) Cancer statistics, 2012. *CA Cancer J Clin* 62:10–29
2. Avallone A, Delrio P, Guida C et al (2006) Biweekly oxaliplatin, raltitrexed, 5-fluorouracil and folinic acid combination chemotherapy during preoperative radiation therapy for locally advanced rectal cancer: a phase I-II study. *Br J Cancer* 94:1809–1815
3. Janjan NA, Crane C, Feig BW et al (2001) Improved overall survival among responders to preoperative chemoradiation for locally advanced rectal cancer. *Am J Clin Oncol* 24:107–112
4. Beets-Tan RG, Beets GL (2004) Rectal cancer: review with emphasis on MR imaging. *Radiology* 232:335–346
5. Leach MO, Brindle KM, Evelhoch JL et al (2005) The assessment of antiangiogenic and antivascular therapies in early-stage clinical trials using magnetic resonance imaging: issues and recommendations. *Br J Cancer* 92:1599–1610
6. Salmo E, El-Dhuwaib Y, Haboubi NY (2010) Histological grading of tumour regression and radiation colitis in locally advanced rectal cancer following neo-adjuvant therapy; a critical appraisal. *Color Dis*. doi:10.1111/j.1463-1318.2010.02412.x
7. Daniel BL, Yen YF, Glover GH et al (1998) Breast disease: dynamic spiral MR imaging. *Radiology* 209:499–509
8. Gollub MJ, Gultekin DH, Akin O, Do RK, Fuqua JL 3rd, Gonen M et al (2012) Dynamic contrast enhanced-MRI for the detection of pathological complete response to neoadjuvant chemotherapy for locally advanced rectal cancer. *Eur Radiol* 22:821–831
9. Petrillo A, Fusco R, Petrillo M, Granata V, Filice S, Delrio P et al (2014) Dynamic contrast enhanced-MRI in locally advanced rectal cancer: value of time intensity curve visual inspection to assess neo-adjuvant therapy response. *J Physiol Health* 110:255–267
10. Hong HS, Kim SH, Park HJ, Park MS, Kim KW, Kim WH et al (2013) Correlations of dynamic contrast-enhanced magnetic resonance imaging with morphologic, angiogenic, and molecular prognostic factors in rectal cancer. *Yonsei Med J* 54:123–130
11. Bajpai J, Gamanagatti S, Sharma MC, Kumar R, Vishnubhatla S, Khan SA et al (2010) Noninvasive imaging surrogate of angiogenesis in osteosarcoma. *Pediatr Blood Cancer* 54:526–531
12. Zhang XM, Yu D, Zhang HL et al (2008) 3D dynamic contrast-enhanced MRI of rectal carcinoma at 3T: correlation with microvascular density and vascular endothelial growth factor markers of tumor angiogenesis. *J Magn Reson Imaging* 27:1309–1316
13. Knopp MV, Weiss E, Sinn HP et al (1999) Pathophysiologic basis of contrast enhancement in breast tumors. *J Magn Reson Imaging* 10:260–266
14. Pham CD, Roberts TP, van Bruggen N et al (1998) Magnetic resonance imaging detects suppression of tumor vascular permeability after administration of antibody to vascular endothelial growth factor. *Cancer Investig* 16:225–230
15. Fusco R, Sansone M, Maffei S, Petrillo A (2012) Dynamic contrast-enhanced MRI in breast cancer: a comparison between distributed and compartmental tracer kinetic models. *J Biomed Graph Comput* 2:23–36
16. Evelhoch JL (1999) Key factors in the acquisition of contrast kinetic data for oncology. *J Magn Reson Imaging* 10:254–259
17. Fusco R, Petrillo A, Petrillo M, Sansone M (2013) Use of tracer kinetic models for selection of semi-quantitative features for DCE-MRI data classification. *Appl Magn Reson* 44:1311–1324
18. Guo JY, Reddick WE (2009) DCE-MRI pixel-by-pixel quantitative curve pattern analysis and its application to osteosarcoma. *J Magn Reson Imaging* 30:177–184
19. Avallone A, Delrio P, Pecori B et al (2011) Oxaliplatin plus dual inhibition of thymidilate synthase during preoperative pelvic radiotherapy for locally advanced rectal carcinoma: long-term outcome. *Int J Radiat Oncol Biol Phys* 79:670–676

20. Petrillo A, Catalano O, Delrio P et al (2007) Post-treatment fistulas in patients with rectal cancer: MRI with rectal superparamagnetic contrast agent. *Abdom Imaging* 32:328–331
21. Dresen RC, Beets GL, Rutten HJ et al (2009) Locally advanced rectal cancer: MR imaging for restaging after neoadjuvant radiation therapy with concomitant chemotherapy. Part I. Are we able to predict tumor confined to the rectal wall? *Radiology* 252:81–91
22. Andreola S, Leo E, Belli F et al (2001) Adenocarcinoma of the lower third of the rectum surgically treated with a <10-mm distal clearance: preliminary results in 35 N0 patients. *Ann Surg Oncol* 8:611–615
23. Mandard AM, Dalibard F, Mandard JC, Mamay J, Henry-Amar M, Petiot JF et al (1994) Pathologic assessment of tumor regression after preoperative chemoradiotherapy of esophageal carcinoma. Clinicopathologic correlations. *Cancer* 73:2680–2686
24. Obuchowski NA (2005) ROC analysis. *AJR Am J Roentgenol* 184:364–372
25. De Long ER, DeLong DM, Clarke-Pearson DL (1988) Comparing the areas under two or more correlated receiver operating characteristic curves: a nonparametric approach. *Biometrics* 44:837–845
26. Schisterman EF, Perkins NJ, Liu A, Bondell H (2005) Optimal cut-point and its corresponding Youden Index to discriminate individuals using pooled blood samples. *Epidemiology* 16:73–81
27. Schabel MC, Morrell GR, Oh KY, Walczak CA, Barlow RB, Neumayer LA (2010) Pharmacokinetic mapping for lesion classification in dynamic breast MRI. *J Magn Reson Imaging* 31:1371–1378
28. Lavini C, de Jonge MC, van de Sande MG, Tak PP, Nederveen AJ, Maas M (2007) Pixel-by-pixel analysis of DCE MRI curve patterns and an illustration of its application to the imaging of the musculoskeletal system. *Magn Reson Imaging* 25:604–612
29. Tuncbilek N, Karakas HM, Altaner S (2004) Dynamic MRI in indirect estimation of microvessel density, histologic grade, and prognosis in colorectal adenocarcinomas. *Abdom Imaging* 29:166–172
30. Blomqvist L, Fransson P, Hindmarsh T (1998) The pelvis after surgery and radio-chemotherapy for rectal cancer studied with Gd-DTPA-enhanced fast dynamic MR imaging. *Eur Radiol* 8:781–787
31. Kim SH, Lee JM, Gupta SN, Han JK, Choi BI (2014) Dynamic contrast-enhanced MRI to evaluate the therapeutic response to neoadjuvant chemoradiation therapy in locally advanced rectal cancer. *J Magn Reson Imaging* 40:730–737
32. Hötter AM, Schmidtman I, Oberholzer K, Düber C (2014) Dynamic contrast enhanced-MRI in rectal cancer: inter- and intraobserver reproducibility and the effect of slice selection on pharmacokinetic analysis. *J Magn Reson Imaging* 40:715–722
33. Intven M, Reerink O, Philippens ME (2014) Dynamic contrast enhanced MR imaging for rectal cancer response assessment after neoadjuvant chemoradiation. *J Magn Reson Imaging* Aug 14
34. Lim JS, Kim D, Baek SE, Myoung S, Choi J, Shin SJ et al (2012) Perfusion MRI for the prediction of treatment response after preoperative chemoradiotherapy in locally advanced rectal cancer. *Eur Radiol* 22:1693–1700
35. Park MJ, Kim SH, Lee SJ, Jang KM, Rhim H (2011) Locally advanced rectal cancer: added value of diffusion-weighted MR imaging for predicting tumor clearance of the mesorectal fascia after neoadjuvant chemotherapy and radiation therapy. *Radiology* 260:771–780
36. Curvo-Semedo L, Lambregts DM, Maas M, Thywissen T, Mehsen RT, Lammering G et al (2011) Rectal cancer: assessment of complete response to preoperative combined radiation therapy with chemotherapy—conventional MR volumetry versus diffusion-weighted MR imaging. *Radiology* 260:734–743
37. DeVries AF, Kremser C, Hein PA et al (2003) Tumor microcirculation and diffusion predict therapy outcome for primary rectal carcinoma. *Int J Radiat Oncol Biol Phys* 56:958–965
38. Cai PQ, Wu YP, An X, Qiu X, Kong LH, Liu GC et al (2014) Simple measurements on diffusion-weighted MR imaging for assessment of complete response to neoadjuvant chemoradiotherapy in locally advanced rectal cancer. *Eur Radiol* 24:2962–2970
39. Genovesi D, Filippone A, Ausili Cēfaro G, Trignani M, Vinciguerra A, Augurio A et al (2013) Diffusion-weighted magnetic resonance for prediction of response after neoadjuvant chemoradiation therapy for locally advanced rectal cancer: preliminary results of a monoinstitutional prospective study. *Eur J Surg Oncol* 39:1071–1078
40. Wu LM, Zhu J, Hu J, Yin Y, Gu HY, Hua J et al (2013) Is there a benefit in using magnetic resonance imaging in the prediction of preoperative neoadjuvant therapy response in locally advanced rectal cancer? *Int J Colorectal Dis* 28:1225–1238
41. Song I, Kim SH, Lee SJ, Choi JY, Kim MJ, Rhim H (2012) Value of diffusion-weighted imaging in the detection of viable tumour after neoadjuvant chemoradiation therapy in patients with locally advanced rectal cancer: comparison with T2 weighted and PET/CT imaging. *Br J Radiol* 85:577–586
42. Cascini GL, Avallone A, Delrio P, Guida C, Tatangelo F, Marone P et al (2006) 18F-FDG PET is an early predictor of pathologic tumor response to preoperative radiochemotherapy in locally advanced rectal cancer. *J Nucl Med* 47:1241–1248
43. Veronesi G, Landoni C, Pelosi G et al (2002) Fluoro-deoxy-glucose uptake and angiogenesis are independent biological features in lung metastases. *Br J Cancer* 86:1391–1395